Title

Ultrasound biomicroscopy of the equine iridocorneal angle

Journal

Equine Veterinary Journal, 54(6)

ISSN

0425-1644

Authors

Knickelbein, Kelly E

Lassaline, Mary E

Kim, Soohyun

et al.

Publication Date

2022-11-01

DOI

10.1111/evj.13585

Peer reviewed

HHS Public Access

Author manuscript

Equine Vet J. Author manuscript; available in PMC 2023 November 01.

Published in final edited form as:

Equine Vet J. 2022 November ; 54(6): 1153–1158. doi:10.1111/evj.13585.

Ultrasound biomicroscopy of the equine iridocorneal angle

Kelly E Knickelbein[1,*], **Mary E Lassaline**[2,**], **Soohyun Kim**[1], **Sara M. Thomasy**[2,3]

[1]Veterinary Medical Teaching Hospital, University of California-Davis, Davis, CA, USA

[2]Department of Surgical and Radiological Sciences, School of Veterinary Medicine, University of California-Davis, Davis, CA, USA

[3]Department of Ophthalmology and Vision Science, University of California-Davis, Davis, CA, USA

Summary

Background: The iridocorneal angle (ICA) is the major pathway of aqueous humor outflow from the anterior chamber of the eye. Ultrasound biomicroscopy (UBM) has been utilized to characterize the morphology of this drainage pathway in numerous species. UBM may allow for early recognition of aqueous humor outflow obstructions in horses, allowing for earlier recognition of risk for glaucoma, a vision-threatening and painful disease. UBM morphology of the normal equine ICA has yet to be described.

Objectives: To determine the ultrasonographic morphology of the equine ICA by UBM in standing sedated horses.

Study design: *In vivo* experimental study.

Methods: 30 healthy adult horses underwent UBM of the ICA at 4 locations (superior, temporal, inferior, nasal) of each eye utilizing standing sedation, topical anesthesia, and auriculopalpebral perineural anesthesia. Anatomic structures were defined on ultrasound images through comparison to published histologic photomicrographs of the equine ICA.

Results: Ultrasound imaging of the ICA at all 4 locations was easily performed in standing, sedated horses. High-resolution images of the ICA allowed for identification of the pectinate ligament, corneoscleral trabecular meshwork (TM), uveal TM, and supraciliary TM.

Corresponding author: Kelly E. Knickelbein kek248@cornell.edu.

*Dr. Knickelbein's current affiliation is: Department of Clinical Sciences, College of Veterinary Medicine, Cornell University, Ithaca, NY, USA

**Dr. Lassaline's current affiliation is: Department of Clinical Sciences & Advanced Medicine, University of Pennsylvania School of Veterinary Medicine, Philadelphia, PA, USA

Authorship: K. Knickelbein designed and executed the study, performed image analysis and interpretation, and prepared the manuscript. M. Lassaline aided in study design and reviewed the manuscript. S. Kim aided in study execution and reviewed the manuscript. S. Thomasy aided in study design, execution, and reviewed the manuscript. All authors have full access to and take responsibility for the integrity of the data. K. Knickelbein takes responsibility for the accuracy of data analysis.

Competing interests: The authors have no competing interests to disclose.

Ethical Animal Research: This study was approved by the Institutional Animal Care and Use Committee of the University of California-Davis and was performed in accordance with the Association for Research in Vision and Ophthalmology guidelines on the use of animals in research. All horses were research animals owned by the University of California-Davis.

Main limitations: Pupil size was midrange in all eyes but was not strictly controlled. Lighting conditions not controlled. Various breeds included.

Conclusion: *In vivo* UBM of the equine ICA is feasible and provides high-resolution images of the structures of the aqueous humor outflow pathway.

Keywords

UBM; horse; eye; glaucoma; aqueous humor

Introduction

The iridocorneal angle (ICA) of the eye is a complex structure through which aqueous humor exits the anterior chamber. Obstruction of aqueous humor outflow at this location is a common cause of ocular hypertension and resultant glaucoma, a blinding and painful disease. Despite glaucoma being a consistently recognized and difficult to manage vision-threatening ocular disease in horses, tools for early detection and effective long-term treatment are lacking. Though most commonly attributed to equine recurrent or chronic uveitis, non-uveitic glaucomas including congenital, primary, and senile glaucoma occur in horses and are likely underdiagnosed.[1–6]

While tonometry remains the most utilized diagnostic to assess for glaucoma, intraocular pressure elevation occurs at late stages of obstruction of aqueous humor outflow, and tools to assess for early aqueous humor outflow obstruction are needed. Early assessment of risk for glaucoma could allow for implementation of interventions that may prolong vision and comfort. Ultrasound biomicroscopy (UBM) has been utilized to assess the morphology of the ICA in numerous species including rabbits,[7] dogs,[8–13] and people.[14,15] Use of UBM to evaluate risk for intraocular pressure elevations and mechanisms of glaucoma is becoming more prevalent in veterinary ophthalmology.[16–18]

The objective of this study was to determine the feasibility of performing UBM to assess the morphology of the ICA in standing sedated horses. Additionally, this study aimed to identify anatomic structures of the ICA visible on the resultant high-resolution ultrasonographic images. Finally, the study aimed to produce reference images of normal equine ICAs for comparison to clinical cases.

Materials and Methods

Animals

A previous study identified minimal variation in measurements of central corneal thickness obtained via UBM in a sample of 50 eyes of juvenile horses of varying ages.[19] Based on this and the expectation that there would be less variation in interindividual ocular parameters of fully mature horses, a sample of 60 eyes was predicted to provide an adequate sample size for determination of normal morphology of the equine anterior segment as determined by UBM.

Thirty healthy adult research horses (15 mares, 15 geldings) with a mean age 14.4 ± 5.0 years of various breeds (Thoroughbred (12), Quarter Horse (12), Warmblood (3), American Paint Horse (2), and Lusitano (1)) were included. Horses were group-housed on dry lots and all resided at the same facility. Medical history was known for all horses and none had prior documentation of ocular disease. Included horses had no evidence of ocular disease on complete ophthalmic examination including pre- and post-dilation slit lamp biomicroscopy with an SL-17 Portable Slit Lamp[a] and indirect ophthalmoscopy using a 14-diopter condensing lens[b]. Intraocular pressures were estimated using rebound tonometry with a TonoVet Plus®[c], and were within the range of 15–25 mmHg in both eyes of all horses. The complete ophthalmic examination to determine inclusion was performed at least 7 days prior to image acquisition. Pupillary dilation for this examination was achieved with 1% tropicamide ophthalmic solution[d], which has a duration of 12 hours in horses.[20] No pupils remained dilated at the time of UBM image acquisition. Intraocular pressure was re-assessed in all eyes on the day of UBM image acquisition and remained within the range of 15–25mmHg in all included eyes.

Ultrasound biomicroscopy and image analysis

Horses were sedated with intravenous detomidine hydrochloride[e] (0.01 mg/kg intravenously) and positioned with their head on a stand with the head above the heart in a normal carriage position. Auriculopalpebral perineural anesthesia was performed bilaterally with 2% lidocaine hydrochloride[f]. Corneal anesthesia was provided with 0.5% tetracaine hydrochloride[g]. The eyelids were manually retracted. Imaging was performed in a covered barn, though lighting conditions were not directly controlled. Pupil size was assessed as midrange in all horses and no mydriatic nor miotic medications were utilized. Images were acquired by one of two authors (KEK or SK) with each author performing imaging on fifteen horses.

A commercially available ultrasound biomicroscope Compact Touch STS UBM[h], with a 50-MHz linear transducer probe fitted with a ClearScan® probe cover[i] filled with sterile water was used to acquire images of both eyes of each included horse. Optixcare® Eye Lube[j], was used as a coupling agent. Transcorneal ultrasonography was performed and images of the superior, temporal, inferior, and nasal iridocorneal angle were obtained in triplicate. The probe was oriented perpendicular to the limbus and placed perpendicular to the globe such that the corneal epithelium, Descemet's membrane, and anterior lens capsule were of similar echogenicity ensuring a non-obliqued image. Acquired ultrasound images were reviewed and compared to published histologic photomicrographs[21,22] of the equine ICA for anatomic structure identification.

Manufacturers' addresses
[a] Kowa Optimed Inc., Torrance, CA, USA
[b] Volk, Mentor, OH, USA
[c] iCare Finland Oy, Helsinki, Finland
[d] Alcon Laboratories Inc., Fort Worth, TX, USA
[e] Dormosedan®, Zoetis Inc., Parsippany, NJ, USA
[f] VetOne, Boise, ID, USA
[g] Bausch & Lomb, Tampa, FL, USA
[h] Quantel Medical, France
[i] ESI Inc., Plymouth, MN, USA
[j] CLC MEDICA, Ontario, Canada

Results

High-resolution images of the superior, temporal, inferior, and nasal iridocorneal angle were readily obtained in each eye of each included horse. Images of the superior and temporal regions of the ICA were easiest to obtain with minimal manual eyelid retraction (Fig. 1). The nasal and inferior regions of the ICA were on occasion slightly more challenging to image due to skull conformation and the position of the inferior and third eyelids. However, it was possible to acquire images in all horses at these locations by tilting the head (ipsilateral ear towards examiner, nose away from examiner) and further manually retracting the inferior eyelid. Image acquisition was well-tolerated in all horses.

Identifiable structures within the ICA included the pectinate ligament, corneoscleral trabecular meshwork, uveal trabecular meshwork, and the supraciliary trabecular meshwork (Fig. 2). The ultrasonographic appearance of the ICA differed based on the region in which the images were obtained. The nasal and temporal ICA had very similar morphology which differed slightly in appearance from that of the superior and inferior ICA (Fig 3). In the superior and inferior regions, the corneoscleral junction (limbus) has a less acute angle, and the scleral portion of the limbus extends further axially than it does temporally and nasally. A regionally similar morphologic appearance to the ICA at each of the examined locations was identified in all sixty eyes of the thirty included horses, indicating minimal structural variability of the equine ICA in normal eyes. Additional structures that were reliably imaged included the third eyelid (nasal and inferior locations), cornea, sclera, anterior chamber, iris, corpora nigra (superior and inferior locations) and lens.

Discussion

The present study identified that *in vivo* UBM imaging of the equine ICA is feasible and noninvasive, allowing for evaluation of structures in high-resolution that were previously only assessable histologically following enucleation. The pectinate ligament, corneoscleral trabecular meshwork, uveal trabecular meshwork, and supraciliary trabecular meshwork were repeatedly identifiable using UBM in sedated horses. The regionally similar morphologic appearance of the ICA at each of the examined locations in all the study horses suggests that there is not a high degree of variability in the general ultrasonographic appearance of the ICA in clinically normal horses. Additionally, image acquisition was performed by two different examiners with very similar results, indicating that consistency of images across examiners is achievable. As such, detection of major morphologic differences from these representative images can be interpreted as abnormal. Imaging of the ICA of horses with clinical disease predisposing to aqueous outflow obstruction, ocular hypertension, and glaucoma will be useful in furthering our understanding of the morphologic changes the ICA may undergo in these disease states.

Investigations into the equine aqueous humor outflow pathways began more than 30 years ago with a microsphere model demonstrating outflow via both the conventional (corneoscleral trabecular meshwork → angular aqueous plexus → intrascleral venous plexus) and unconventional (uveal trabecular meshwork → supraciliary space → suprachoroidal space) pathways.[23,24] The histologic features of the normal equine

iridocorneal angle were subsequently described, and the ICA was found to be continuous with a well-defined meshwork of trabeculae between the sclera and ciliary body, termed the supraciliary trabecular meshwork.[21] An additional histologic study confirmed the unique structure of the long and broad trabeculae of the equine pectinate ligament and proposed that due to the robust nature of the pectinate ligament trabeculae and trabecular meshwork, collapse of the ciliary cleft would be practically impossible.[22] A subsequent histologic study on glaucomatous equine globes documented collapse of the ciliary cleft in over 50% of the examined cases,[5] indicating that structural changes to the ICA do occur with glaucoma. Based on the high-resolution images obtained in the present study, such changes should be identifiable *in vivo* using UBM. The ability to document such changes to the ICA early on should allow for earlier implementation of vision-prolonging therapies.

Critical evaluation of the directly visible nasal and temporal aspects of the ICA of the horse remains an important part of the ophthalmic examination. However, this assessment is very limited as the view is segmental and only the anterior-most aspects of the pectinate ligament trabeculae can be seen. UBM provides detailed information about the morphology of the more posterior structures of the ICA and may allow for early recognition of aqueous humor outflow obstructions. UBM imaging of the ICA is applicable for horses with documented elevated intraocular pressure or glaucoma, recurrent or chronic uveitis, corneal edema, and those who will undergo phacoemulsification or other intraocular surgical procedures. Referral to a specialty center with the ability to perform UBM is appropriate for such cases. In addition to imaging of the iridocorneal angle, UBM is also useful for evaluation of ocular surface and anterior segment masses as well as other corneal, scleral, and lens disorders.[9,25] As UBM requires contact with the globe, it should be avoided in fragile globes.

Limitations

A limitation of this study was that lighting conditions and thus pupil size were not strictly controlled, and as such measurements of the iridocorneal angle could not be reliably performed. The peripheral iris, pectinate ligament and adjacent structures of the iridocorneal angle are intimately associated, and as such, pupil size can impact ICA morphology. Images were obtained in horses with a mid-range pupil and the morphology of the ICA in an eye with a miotic or mydriatic pupil may differ. An additional limitation of this study was the inclusion of various breeds, which may have subtle differences in iridocorneal angle morphology

Conclusions

Utilization of UBM to assess the equine ICA is a practical technique that provides high-resolution images of the structures of the aqueous humor outflow pathway. Consistently identifiable structures include the pectinate ligament trabeculae and the corneoscleral, uveal, and supraciliary trabecular meshworks.

Acknowledgements:

The authors acknowledge the UC Davis Center for Equine Health and Monica Motta and Michelle Ferneding for their technical expertise.

Sources of Funding:

American College of Veterinary Ophthalmologists' Vision for Animals Foundation (VAF2019–2), UC Davis RM Cello Endowment, NIH P30 EY12576.

Data availability statement:

The data that support the findings of this study are available from the corresponding author upon reasonable request.

References

1. Wilcock BP, Brooks DE, Latimer CA. Glaucoma in horses. Vet Pathol. 1991;28(1):74–78. doi:10.1177/030098589102800110 [PubMed: 2017829]
2. Cullen CL, Grahn BH. Equine glaucoma: a retrospective study of 13 cases presented at the Western College of Veterinary Medicine from 1992 to 1999. Can Vet J Rev Veterinaire Can. 2000;41(6):470–480.
3. Wilkie DA, Gilger BC. Equine glaucoma. Vet Clin North Am Equine Pract. 2004;20(2):381–391. doi:10.1016/j.cveq.2004.04.002 [PubMed: 15271429]
4. Annear MJ, Gemensky-Metzler AJ, Wilkie DA. Uveitic glaucoma in the horse: Equine glaucoma. Equine Vet Educ. 2012;24(2):97–105. doi:10.1111/j.2042-3292.2011.00310.x
5. Curto EM, Gemensky-Metzler AJ, Chandler HL, Wilkie DA. Equine glaucoma: a histopathologic retrospective study (1999–2012). Vet Ophthalmol. 2014;17(5):334–342. doi:10.1111/vop.12080 [PubMed: 23859597]
6. Henriksen M de L, La Croix N, Wilkie DA, et al. Glaucoma with Descemet's membrane detachment in five horses. Vet Ophthalmol. 2017;20(3):273–279. doi:10.1111/vop.12388 [PubMed: 27191927]
7. Li Puma MC, Freeman KS, Cleymaet AM, et al. Iridocorneal angle assessment of companion rabbits using gonioscopy, spectral-domain optical coherence tomography (Optovue iVue ®), high-resolution ultrasound, and Pentacam ® HR imaging. Vet Ophthalmol. 2019;22(6):834–841. doi:10.1111/vop.12660 [PubMed: 30938083]
8. Gibson TE, Roberts SM, Severin GA, Steyn PF, Wrigley RH. Comparison of gonioscopy and ultrasound biomicroscopy for evaluating the iridocorneal angle in dogs. J Am Vet Med Assoc. 1998;213(5):635–638. [PubMed: 9731256]
9. Bentley E, Miller PE, Diehl KA. Use of high-resolution ultrasound as a diagnostic tool in veterinary ophthalmology. J Am Vet Med Assoc. 2003;223(11):1617–1622. doi:10.2460/javma.2003.223.1617 [PubMed: 14664449]
10. Dulaurent T, Goulle F, Dulaurent A, Mentek M, Peiffer RL, Isard PF. Effect of mydriasis induced by topical instillations of 0.5% tropicamide on the anterior segment in normotensive dogs using ultrasound biomicroscopy: Effect of tropicamide on the anterior segment. Vet Ophthalmol. 2012;15:8–13. doi:10.1111/j.1463-5224.2011.00898.x
11. Park S, Kang S, Lee E, et al. Ultrasound biomicroscopic study of the effects of topical latanoprost on the anterior segment and ciliary body thickness in dogs. Vet Ophthalmol. 2016;19(6):498–503. doi:10.1111/vop.12339 [PubMed: 26709198]
12. Kwak J, Kang S, Lee ER, et al. Effect of preservative-free tafluprost on intraocular pressure, pupil diameter, and anterior segment structures in normal canine eyes. Vet Ophthalmol. 2017;20(1):34–39. doi:10.1111/vop.12341 [PubMed: 26728904]
13. Shim J, Kang S, Jeong Y, Lee E, Jeong D, Seo K. Comparison of iridocorneal angle parameters measured by spectral domain optical coherence tomography and ultrasound biomicroscopy in dogs. Vet Ophthalmol. Published online November 16, 2021:vop.12950. doi:10.1111/vop.12950
14. Ishikawa H, Schuman J. Anterior segment imaging: ultrasound biomicroscopy. Ophthalmol Clin N Am. 2004;17(1):7–20. doi:10.1016/j.ohc.2003.12.001
15. Silverman RH. High-resolution ultrasound imaging of the eye - a review. Clin Experiment Ophthalmol. 2009;37(1):54–67. doi:10.1111/j.1442-9071.2008.01892.x [PubMed: 19138310]

16. Crumley W, Gionfriddo JR, Radecki SV. Relationship of the iridocorneal angle, as measured using ultrasound biomicroscopy, with post-operative increases in intraocular pressure post-phacoemulsification in dogs. Vet Ophthalmol. 2009;12(1):22–27. doi:10.1111/j.1463-5224.2009.00669.x [PubMed: 19152594]
17. Boillot T, Rosolen SG, Dulaurent T, et al. Determination of morphological, biometric and biochemical susceptibilities in healthy Eurasier dogs with suspected inherited glaucoma. PloS One. 2014;9(11):e111873. doi:10.1371/journal.pone.0111873 [PubMed: 25380252]
18. Hasegawa T, Kawata M, Ota M. Ultrasound biomicroscopic findings of the iridocorneal angle in live healthy and glaucomatous dogs. J Vet Med Sci. 2016;77(12):1625–1631. doi:10.1292/jvms.15-0311 [PubMed: 26212256]
19. Herbig LE, Eule JC. Central corneal thickness measurements and ultrasonographic study of the growing equine eye. Vet Ophthalmol. 2015;18(6):462–471. doi:10.1111/vop.12252 [PubMed: 25623263]
20. Gelatt KN, Gum G, MacKay EO. Evaluation of mydriatics in horses. Prog Vet Comp Ophthalmol. 1995;5:104–108.
21. Samuelson D, Smith P, Brooks D. Morphologic features of the aqueous humor drainage pathways in horses. Am J Vet Res. 1989;50(5):720–727. [PubMed: 2729716]
22. Geest JP, Lauwers H, Simoens R, Schaepdrijver L. The morphology of the equine iridocorneal angle: a light and scanning electron microscopic study. Equine Vet J. 2010;22(S10):30–35. doi:10.1111/j.2042-3306.1990.tb04708.x
23. Smith PJ, Samuelson DA, Brooks DE, Whitley RD. Unconventional aqueous humor outflow of microspheres perfused into the equine eye. Am J Vet Res. 1986;47(11):2445–2453. [PubMed: 3789508]
24. Ninomiya H, Inomata T. Functional Microvascular Anatomy of the Horse Eye: A Scanning Electron Microscopic Study of Corrosion Casts. Open J Vet Med. 2014;04(05):91–101. doi:10.4236/ojvm.2014.45011
25. Keenan AV, Townsend WM. Evaluation of equine corneal disease using ultrasound biomicroscopy. Vet Ophthalmol. Published online March 11, 2021:vop.12881. doi:10.1111/vop.12881

Figure 1.
Photograph depicting the Compact Touch STS UBM 50 MHz linear transducer fitted with a ClearScan® probe cover filled with sterile water applied to the equine eye. The horse is sedated with the head resting on a head stand, topical and auriculopalpebral perineural anesthesia have been applied, and the eyelids are gently manually retracted.

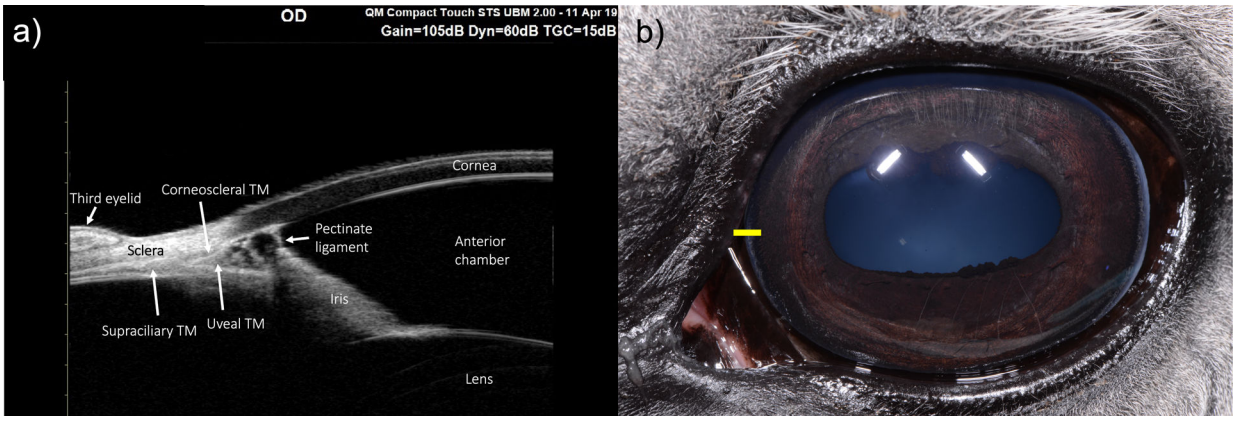

Figure 2.

Representative ultrasound biomicroscopy image of the nasal iridocorneal angle (a) of the eye of a normal adult horse obtained at the location of the yellow line indicated in the clinical image (b). The trabeculae of the pectinate ligament are clearly identifiable, as are the corneoscleral, uveal, and supraciliary trabecular meshwork (TM). Note that at this nasal location the third eyelid is within view but does not interfere with imaging of the ICA. In (b), note that the anterior aspect of the pectinate ligament is visible nasally and temporally but cannot be seen superiorly and inferiorly. The pupil was midrange.

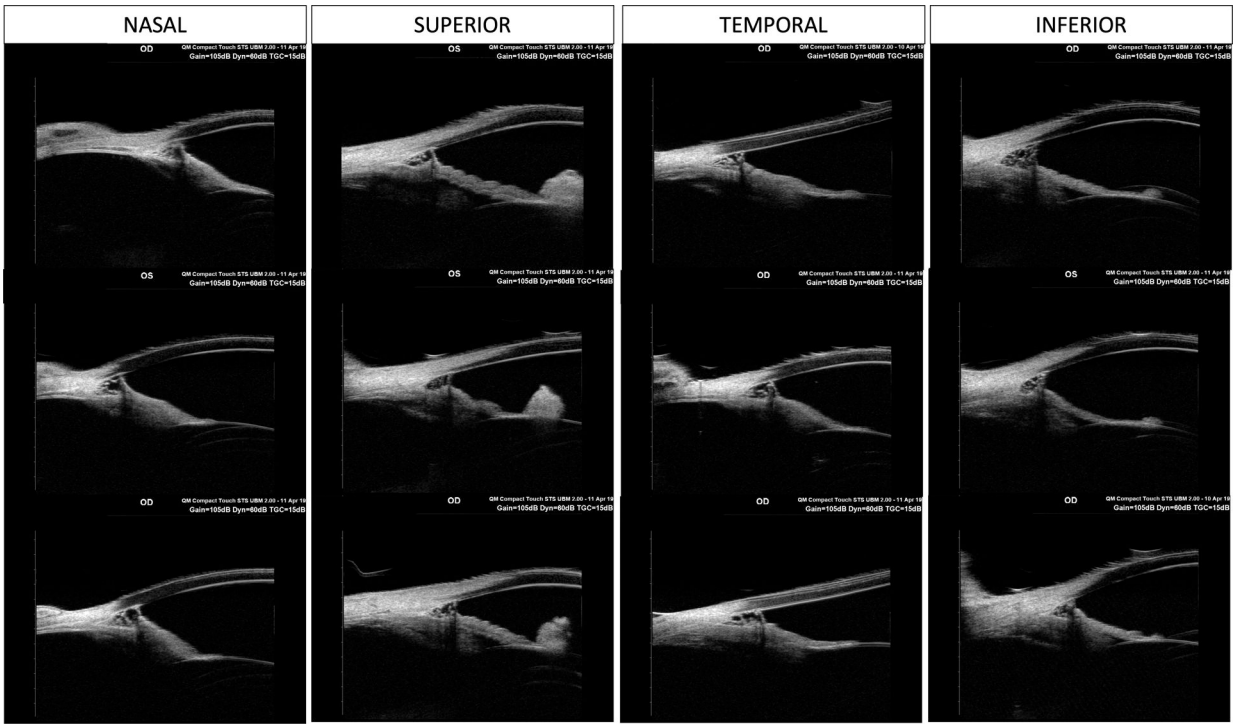

Figure 3.

Representative ultrasound biomicroscopy images of the nasal, superior, temporal, and inferior iridocorneal angle of the normal adult horse. Images from three different horses are included to demonstrate subtle individual differences in morphology. Note that in the superior and inferior images, the corneoscleral junction (limbus) extends further axially than in the nasal and temporal locations. The corpora nigra are seen in the superior and inferior locations. The pupil was midrange.